International Journal of Pattern Recognition
and Artificial Intelligence
Vol. 33, No. 3 (2019) 1955004 (14 pages)

DOI: 10.1142/S0218001419550048

World Scientific
www.worldscientific.com

An Accurate Illumination Model of Machined Surface Based on Micro-Image

Weichao Shi*, Jianming Zheng†, Yan Li‡,
Xubo Li§ and Qiannan An¶

Xi'an University of Technology
Xi'an 710048, P. R. China
**shiweichao@xaut.edu.cn*
†*zjm@xaut.edu.cn*
‡*jyxy-ly@xaut.edu.cn*
§*qqlixubo@126.com*
¶*1532482823@qq.com*

Received 24 May 2018
Accepted 25 July 2018
Published 12 September 2018

This paper focused on the illumination model of machined surface based on micro-image. According to micro-image forming condition, the theory that the image brightness is related to the microfacet topography and surface reflection characteristics is presented. The distribution rule of micro-topography and reflection characteristics of sample surface is analyzed according to the measured data. An illumination mode of machined surface is established based on the analysis result, and the model parameters are obtained by using the simulated annealing algorithm. Verification results show that this proposed model can improve the simulation accuracy significantly and describe the lighting effect of machined surface. The research will provide a new idea and method for the 3D reconstruction.

Keywords: 3D reconstruction; illumination model; machined surface; micro-topography.

1. Introduction

In recent years, three-dimensional reconstruction has played an important role in the development of intelligent recognition field[4,5] which can construct 3D shapes of object from images and estimate the geometric dimensioning of object.[17] As one of the most critical components in 3D reconstruction system, the illumination model can use mathematical or physical methods to describe the lighting phenomenon on the object surface, and establish the relationship between the image gray and the shape of the object surface.[20,23] Therefore, illumination mode has been attracting much attention in 3D reconstruction.[1,10]

† Corresponding author.

As is well known, most of the existing illumination models are based on geometric optical theory, and can describe the lighting effect of the macroscopic rough surface.[15] Bouknight proposed the first optical reflection model, which consists of Lambert diffuse reflection and ambient light.[2] Phong has proposed the famous Phong model, which can approximately describe the specular reflection phenomenon. However, when the incident angle of light is greater than a certain value, it will produce simulated distortion.[13] Torrance and Sparrow put forward the microfacet theory and establish the Torrance–Sparrow model, studying the influence of the spatial position of light source on the specular reflection components.[3,18] Oren and Nayar proposed an Oren–Nayar model suitable for rough surface according to the influence of the light source on the diffuse reflection component, which assumed the rough surface as v-shaped structure.[11] Due to different reflection components being deeply studied in the above illumination models, most of the scholars usually recombine the reflection components to obtain the required illumination model.[6,19] However, the machined surfaces are mostly smooth surfaces with prominent specular reflection. Therefore, the existing light model cannot be used to simulate its lighting effect accurately.

This paper focused on the illumination model of machined surface based on micro-image. The micro-topography and corresponding images of turning sample and plain milled sample were collected by confocal laser scanning microscope, and the micro-topography distribution rules of microfacets and reflection characteristics of surface were analyzed. An illumination model for machined surface is established, and simulated annealing algorithm is used to determine the model parameters. The accuracy of the aforesaid model is verified through a comparison of the model calculating results and measured results. The illumination model can not only depict the micro-topography distribution of the surfaces of same roughness under the same processing conditions, but also simulate the lighting effect of different machined surfaces.

2. Mechanism of Micro-Image Forming

As shown in Fig. 1, under the micro-imaging condition, incident beam is effectively irradiated on the microfacets $dA1$ *and* $dA2$ through the lens and semi-reflecting specular. Due to the microfacets $dA1$ *and* $dA2$ having different topography, the light reflected by the microfacets enters into the imaging optical path after passing the lens, and form different brightness on image pixel 1 and pixel 2.

According to the above principle, with laser as the light source, the angle between the incident light irradiated on the microfacets and the optical axis is very small. It can be assumed that the incident light irradiates the material surface vertically and the intensity of incident light is far greater than the intensity of ambient light. Therefore, the influence of spatial position of the light source on the image brightness can be neglected. The reflection of incident light on the microfacet varies with topography, and so does corresponding image brightness. Under fixed magnification

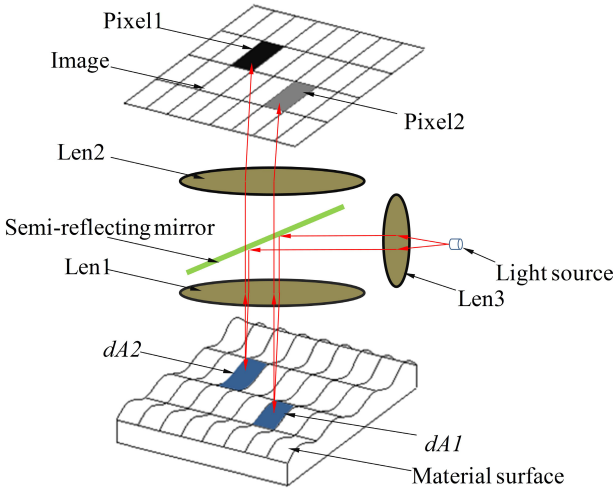

Fig. 1. The principle of micro-imaging.

times of the system, flatter topography of the microfacet can cause the reflection of incident light to be dominated by specular reflection and bring in brighter images; and more irregular topography of the microfacet will bring in overwhelming diffuse reflection of the incident light and less bright images. Therefore, the image brightness is related to the microfacet topography $z(x, y)$ and surface reflection characteristics $f_r(x, y)$.

$$I(x, y) = f(z(x, y), f_r(x, y)). \tag{1}$$

Based on the above assumption, $\mathbf{L}$ (0, 0, 1) is the vector of incident light, and $\mathbf{n}$ $(p, q, -1)$ is the vector of microfacet. The normal declination angle of microfacet θ is the angle between the vector of incident light and the vector of microfacet, which can describe the microfacet topography $z(x, y)$, as shown in Fig. 2.

Therefore, the normal declination angle θ can be calculated by

$$\cos\theta = \frac{1}{\sqrt{1 + p^2 + q^2}}, \tag{2}$$

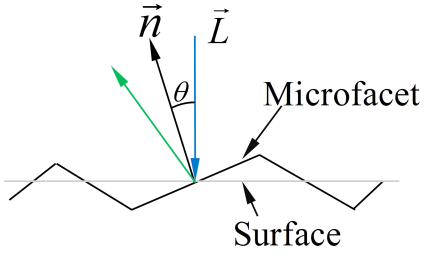

Fig. 2. The normal declination angle.

where p and q can be expressed as

$$\begin{cases} p(x,y) = z(x,y)_x \\ q(x,y) = z(x,y)_y. \end{cases} \tag{3}$$

Therefore, the image brightness $I(x,y)$ can be expressed as

$$I(x,y) = f(\theta(x,y), f_r(x,y)). \tag{4}$$

3. Analysis of Machined Surface Characteristics

3.1. *Measuring equipment*

The experimental platform consists of a confocal microscopy with 10 × object lens (Leica DCM-3D) and an active damping platform, as shown in Fig. 3(a). The turning and plain milled samples of Ra3.2, Ra1.6 and Ra0.8 μm were adopted as the research objects under identical measurement conditions, as shown in Figs. 3(b) and 3(c). The measured data are processed on a computer with Quad-Core processors. The measurement area with $1.25 \times 0.95\,\text{mm}^2$ was measured and the images with a resolution of 768×576 pixels were collected.

3.2. *Measuring data*

The micro-topography and corresponding image are shown in Fig. 4.

Figure 4 shows that the data of topography and image has lots of noise points. The micro-topography has significant characteristics of peak and valley, and corresponding image has feature of alternation of dark and bright. With rising surface roughness, the peak-valley interval increases, and the streak continuity and

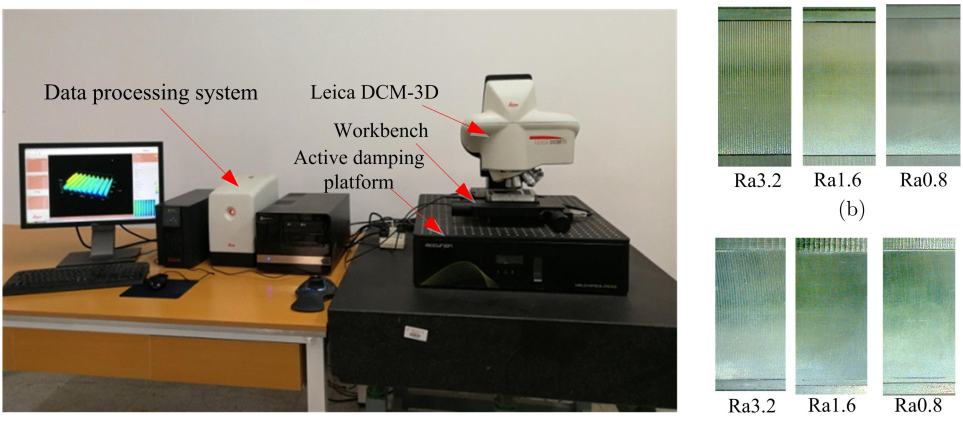

Fig. 3. (a) Measuring equipment, (b) Turning samples and (c) Plain milled samples.

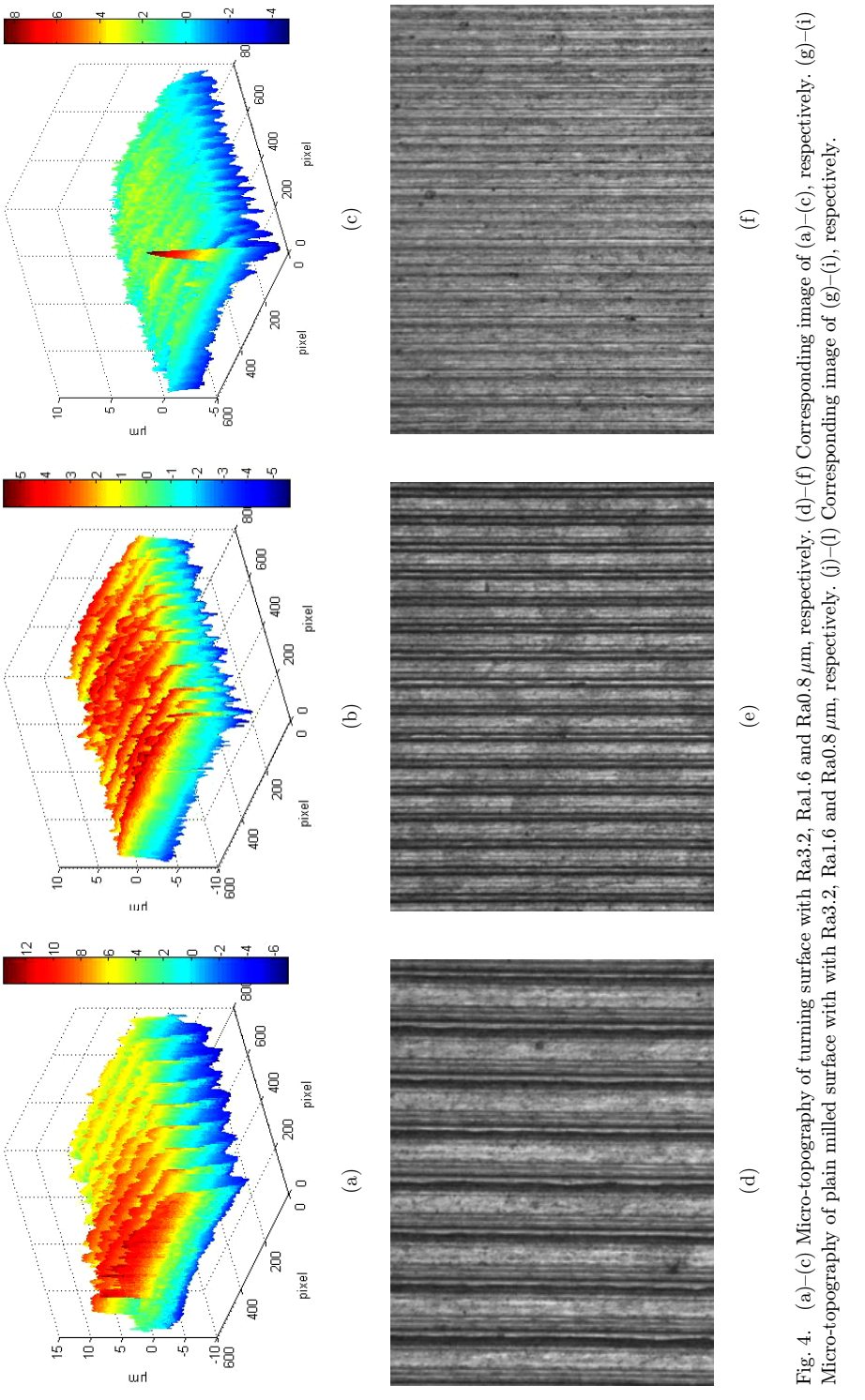

Fig. 4. (a)–(c) Micro-topography of turning surface with Ra3.2, Ra1.6 and Ra0.8 μm, respectively. (d)–(f) Corresponding image of (a)–(c), respectively. (g)–(i) Micro-topography of plain milled surface with with Ra3.2, Ra1.6 and Ra0.8 μm, respectively. (j)–(l) Corresponding image of (g)–(i), respectively.

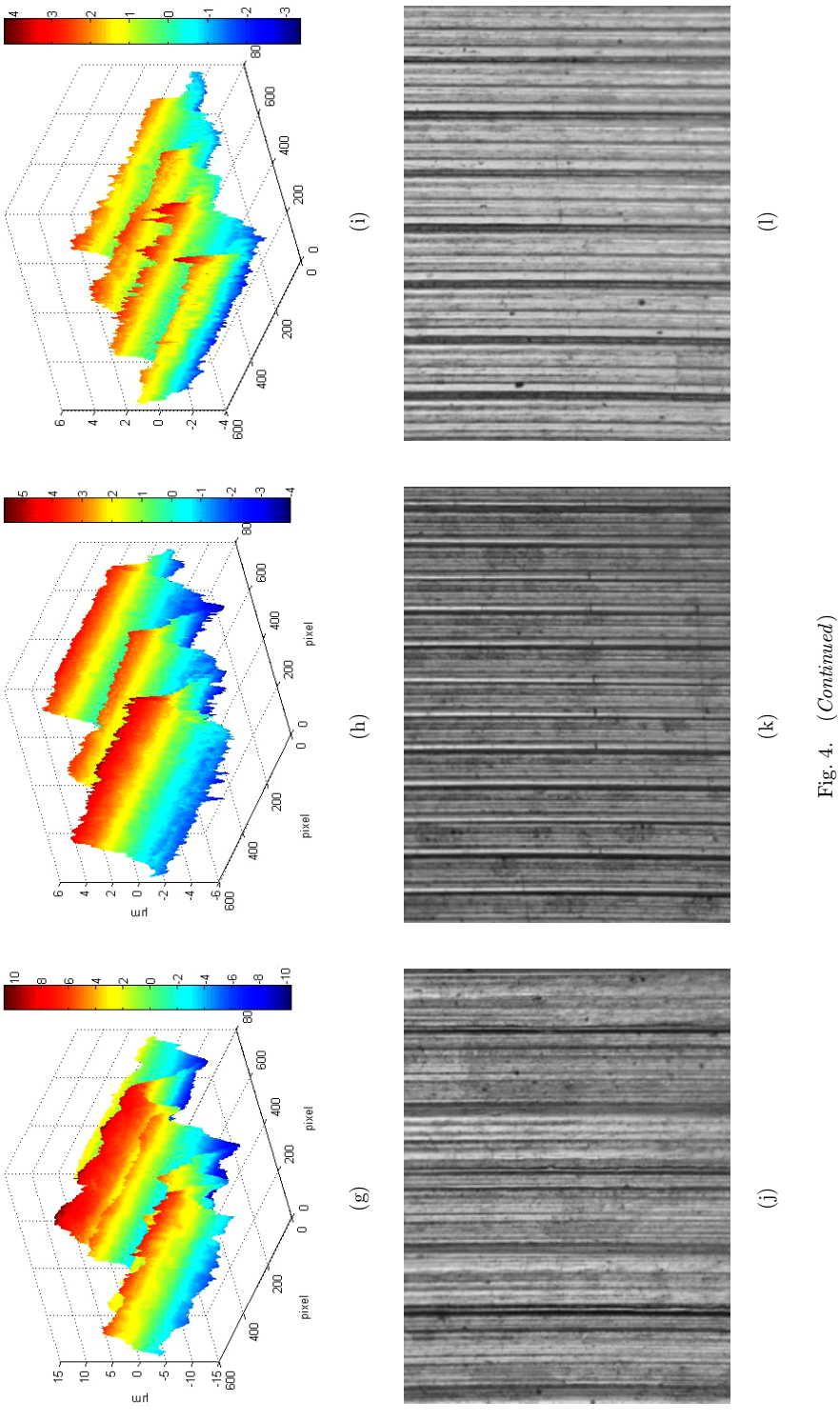

Fig. 4. (*Continued*)

regularity also become more significant. The aforesaid rules indicate close relationship between the surface lighting change and the roughness and topography.

3.3. *Analysis of measuring results*

The measured data of turning and plain milled sample surface of Ra3.2 μm and Ra0.8 μm are extracted for studying the features of the samples surface. Firstly, the trend term of topography data is processed by the least square method to eliminate baseline offset in linear state,[12] the measured data is de-noised through median filter and the image brightness are normalized.[8] Then, the feature points of two sets data are extracted separately to carry out selection and matching of corresponding points. Next, the topography data is rectified with reference image data through iterative closest point (ICP) to complete the rectification of spatial location of two sets of data.[22] Finally, the distribution rules of normal declination angles are performed, and the surface reflection characteristics are analyzed.

3.3.1. *Distribution of the normal declination angle of microfacets*

Since the normal declination angle of the microfacet is helpful in revealing the micro-topography characteristics of the sample surface, it is possible to complete the statistics on the distribution of normal surface declination angles according to the measured data of micro-topography, as shown in Fig. 5.

Figure 5 illustrates that the normal declination angle of microfacets vary with the roughness. The normal declination angle of microfacets is quite diffusive for the surface of Ra3.2 μm with great roughness, but more centralized for the surface of Ra0.8 μm with low roughness. It indicates that with decreasing surface roughness, the normal declination angle of microfacets tends to be more centralized. In addition, the distribution curves of normal declination angles appear to be

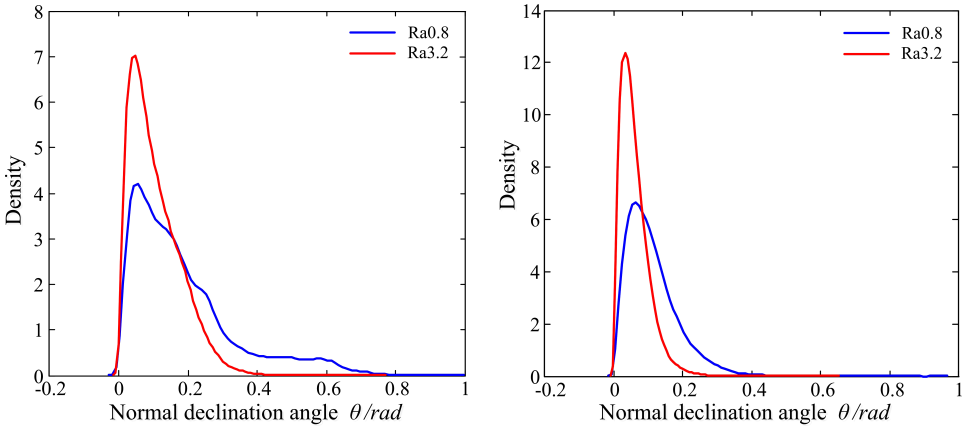

Fig. 5. (a) Turning surface. (b) Plain milled surface.

left–right asymmetry, with the change in right side being more smooth. A fitting analysis of the distribution of normal declination angles on sample surface displays the feature of lognormal distribution.

3.3.2. *Reflectance characteristics of machined surface*

The measuring method of bidirectional reflectance distribution function (BRDF) is used in the investigation.[16] The measuring method implies that BRDF measurements can be calculated by image brightness, normal declination angle of microfacet and incident radiance:

$$\mathrm{BRDF} = \frac{L_r}{E_i} = \frac{\eta E}{L_i \cdot dA \cdot \cos\theta}, \tag{5}$$

where E_i is the brightness of image pixel, L_i is the incident radiance, dA is the area of microfacets, and θ is normal declination angle of microfacet.

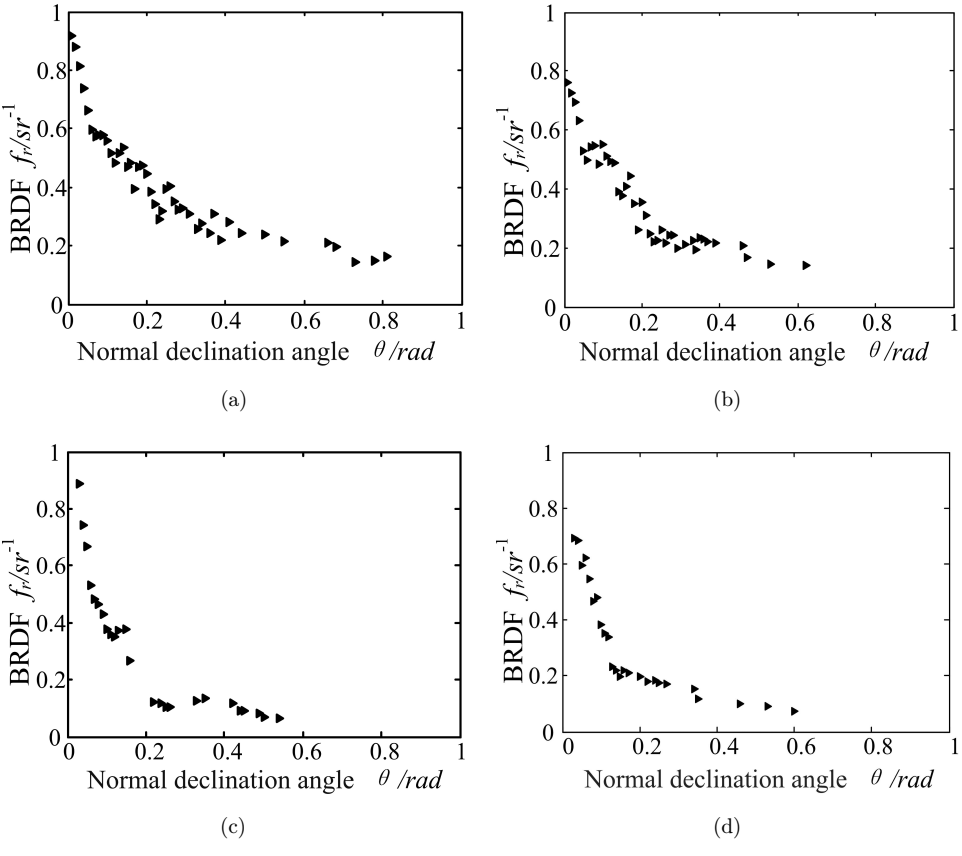

Fig. 6. (a)–(b) Turning surface with Ra3.2 μm, Ra0.8 μm, respectively. (c)–(d) Plain milled surface with Ra3.2 μm, Ra0.8 μm, respectively.

According to the data of topography and corresponding images, the BRDF measurements are calculated by the above formula. The BRDF measurements of sample surface is shown in Fig. 6.

Figure 6 indicates that BRDF measurements grow with the declining normal declination angle of microfacets. The smaller the angle is, the smoother the topography will be, and the more prominent the specular reflection will be. Besides, BRDF distribution rules also vary on different sample surfaces, which are mainly related to the distribution of normal declination angle of microfacets. As for sample of Ra3.2, the normal declination angle of microfacets on the surface is relatively scattered, and so is the BRDF measurements. The reflectance characteristics of machined surface are diffuse reflection and specular reflection, among which the specular reflection is more significant. For sample of Ra 0.8, the distribution of normal declination angles and BRDF measurements are centralized, and its surface reflection is also expressed mainly as specular reflection.

4. Illumination Model

4.1. *Parameter model*

The illumination model of machined surface, which is determined by the properties of the workpiece, is a complicated function of surface topography distribution, light source features and reflection characteristics. According to the condition of micro-image forming, the effect of ambient light on imaging of machined surface can be ignored. It can be inferred from the microfacet theory that with the size of each microfacet on the machined surface being longer than the wavelength of incident light, the diffraction of light can be neglected here. Thus, the illumination model consists of specular reflection model and diffuse reflection model. According to Ward model theory, normalization coefficient is used to substitute the geometrical attenuation factor and Fresnel coefficient.[21] The illumination model of machined surface is established with the distribution rules of normal declination angles and reflection characteristics of the samples as follows:

$$I = \frac{k_d I_{pd}}{\pi} + k_s I_{pd} \frac{\exp[-a * (\mathrm{In}\theta)^2/2\sigma^2]}{4\pi\sigma^2}, \tag{6}$$

where the diffuse reflection model is the first term in Eq. (6), which follows Lambert's law. And the specular reflection model is the second term. σ is the machined surface roughness RMS. $\exp[-a * (\mathrm{In}\theta)^2/2\sigma^2]$ is the distribution function of the normal declination angle of microfacets. $1/4\pi\sigma^2$ is the normalization factor. k_d, k_s and a is the undetermined parameters. k_d and k_s, respectively indicate the diffuse reflection coefficient and specular reflection coefficient, which are related to roughness and reflectivity of machined surface. a reflects the distribution function of the normal declination angle, and relates to the surface micro-topography.

Table 1. The parameters of illumination model.

Machined Method	Roughness Ra (μm)	k_d	k_s	a
Turning	3.2	0.12	0.464	−7.751
	1.6			−7.452
	0.8			−6.924
Plain milled	3.2	0.07	0.221	−20.35
	1.6			−18.75
	0.8			−17.58

4.2. *Data fitting and parameters solving*

The Simulated Annealing Algorithm (SAA) is used to obtain the illumination model parameters, which is a global searching method based on the Monte Carlo iterative computation method.[9] The objective function is obtained as follows:

$$E(k_d, k_s, a) = \sum_{\theta} g(\theta)[I_{\text{model}}(k_d, k_s, a) - I_{\text{measured}}(\theta)]^2 \rightarrow \min \tag{7}$$

where I_{model} is the calculated brightness data; I_{measured} is the measured brightness; $g(\theta)$ is weight function.

According to the above calculation method, the model parameters are shown in Table 1.

5. Illumination Model Validation

To verify the accuracy of the illumination model given in this paper, the Phong model, which can approximately describe the specular reflection, was simplified to obtain its reflection model under the condition of coaxial microscopic imaging:

$$I = k_d I_{pd} \cos\theta + k_s I_{pd} (\cos 2\theta)^n, \tag{8}$$

where n is the highlight index, which can describe the smoothness of the surface. According to the above fitting method, we can determine $n = 100$. The sample surface of turning and plain milled with Ra1.6 μm was simulated by two models. The synthetic image is shown in Fig. 7.

The measurements and simulation results are compared as shown in Fig. 8. Note that the brightness in the figure is normalized in order to facilitate comparison.

It can be seen from Fig. 8 that the specular reflection of proposed model accounts for a higher proportion at the small angles, and the calculation results fit well with the measurements. When the normal declination angle is larger, the error between the calculation results and measurements is larger. This indicates that the specular reflection energy is more concentrated. The proposed model and Phong model are compared. Compared with the measurements, the calculation results of Phong model are larger than the measurements, and the error is larger, which indicates that the Phong model is not suitable for describing smooth surfaces under microscopic

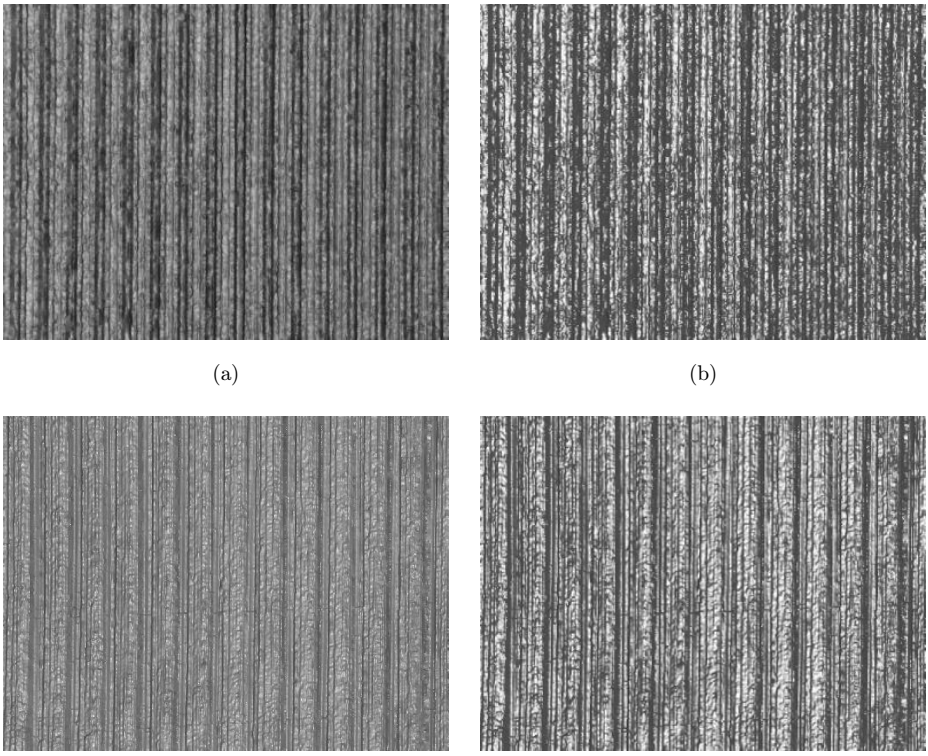

(a) (b)

(c) (d)

Fig. 7. (a) Synthetic image of turning surface using proposed model. (b) Synthetic image of turning surface using Phong model l. (c) Synthetic image of plain milled surface using proposed mode. (d) Synthetic image of plain milled surface using Phong model.

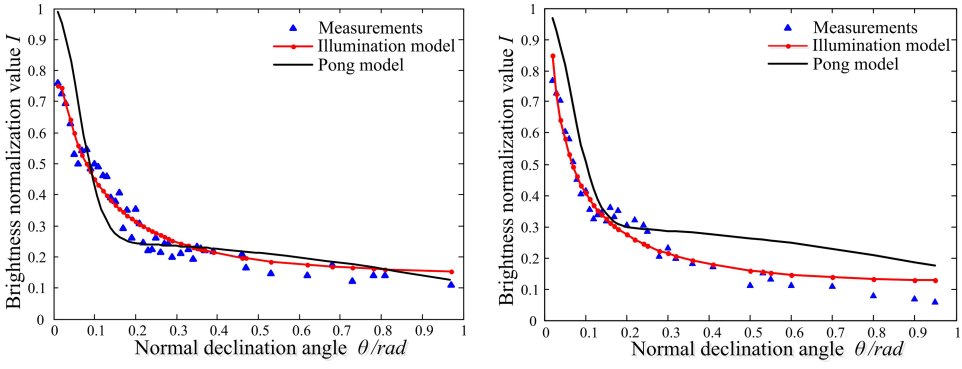

(a) (b)

Fig. 8. (a) Fitting error of turning surface. (b) Fitting error of plain milled surface.

Table 2. The result of RMSE.

Machined Method	Roughness Ra (μm)	RMSE1	RMSE2	Percent Decrease (%)
Turning	1.6	0.972	1.462	49
Plain milled	1.6	0.943	1.605	66.2

conditions. The error can be calculated by using the relative root-mean-square error (RMSE) as follows[7,14]:

$$\sigma = \sqrt{\frac{1}{N}\sum\left(\frac{I_{\text{model}} - I_{\text{measured}}}{I_{\text{measured}}}\right)^2}. \tag{9}$$

According to the calculation results of the two models and the measurements, the RMSE of the proposed model (RMSE1) and RMSE of Phong model (RMSE2) are given in Table 2.

As seen from Table 2, the proposed model significantly improves the calculation accuracy of image brightness, and can describe the lighting effect of machined surface accurately. Although the error between the calculation results of proposed model and measurements still exist at large angles, we will decrease the error in the future.

6. Conclusion

This paper proposes a new illumination model of machined surface based on micro-image. According to the micro-imaging mechanism, the theory that micro-topography and surface reflection characteristics are the effects on image brightness is presented. To obtain the micro-topography data and corresponding image brightness data, sample surface with different roughness were carefully measured. The analysis results of the measured data show that the distribution of micro-topography has the feature of lognormal distribution, and the reflectance characteristics of surface are diffuse reflection and specular reflection. The illumination model is built based on the microfacet theory. Verification results show that the error of the proposed model is smaller than that of the Phong mode, which indicates that the proposed model improves the simulation accuracy significantly and describes the lighting effect of the machined surface. However, the size of samples extracted is small. It needs to increase the size of samples in the future to improve the reliability of the illumination model.

Acknowledgment

This work is supported by Natural Science Foundation Research Project of Shaanxi Province.

References

1. G. Al-Kindi, R. Baul and K. Gill, Experimental evaluation of 'Shape from Shading' for engineering component profile measurement, *Proc. Inst. Mech. Eng. UK* **203**(B) (1989) 211–216.

2. W. Bouknight, A procedure for generation of three dimensional half-toned computer graphic presentations, *Commun. ACM* **13**(9) (1970) 527–536.
3. R. L. Cook and K. E. Torrance, A reflectance model computer graphics, *Comput. Graph.* **15**(4) (1981) 307–316.
4. Z. Du and Y. Du, Simple three-dimensional laser radar measuring method and model reconstruction for hot heavy forgings, *Opt. Eng.* **51**(2) (2012) 021118.
5. H. Gao, L. Liu, Y. Tian and S. Y. Lu, 3D reconstruction for road scene with obstacle detection feedback, *Int. J. Pattern Recognit. Artif. Intell.* **20**(5) (2018) 1454006.
6. H. Hirayama, K. Kaneda, H. Yamashita and Y. Monden, An accurate illumination model for objects coated with multilayer films, *Comput. Graph.* **25**(3) (2001) 391–400.
7. J. E. Hubbs, L. D. Brooks, M. J. Nofziger, F. O. Bartell and W. L. Wolfe, Bidirectional reflectance distribution function of the Infrared Astronomical Satellite solar-shield material, *Appl. Opt.* **21** (1982) 3323–3325.
8. M. R. Islam, X. Chen and H. Yu, A novel weighted variational model for image denoising, *Int. J. Pattern Recognit. Artif. Intell.* **31**(12) (2017) 1751022.
9. F. Jin, S. J. Song and C. Wu, A simulated annealing based beam search algorithm for the flow-shop scheduling problem, *Int. J. Pattern Recogn. Artif. Intell.* **22**(1) (2008) 65–75.
10. I. A. Kakadiaris, G. Toderici and G. Evangleopoulos, 3D-2D face recognition with pose and illumination normalization, *Comput. Vis. Image Underst.* **154**(C) (2017) 137–151.
11. M. Oren and S. K. Nayar, Generalization of the Lambertian model and implications for machine vision, *Int. J. Comput. Vis.* **14** (1995) 227–251.
12. Z. K. Peng, P. W. Tse and F. L. Chu, An improved Hilbert–Huang transform and its application in vibration signal analysis, *J. Sound Vib.* **286**(1–2) (2005) 187–205.
13. B. T. Phong, Illumination for computer generated picture, *Commun. ACM* **18**(6) (1975) 449–455.
14. T. Ren, X. Kang, W. Sun and H. Song, Study of dynamometer cards identification based on root-mean-square error algorithm, *Int. J. Pattern Recogn. Artif. Intell.* **32**(2) (2018) 1850004.
15. C. Schlick, A survey of shading and reflectance models, *Comput. Graph. Forum.* **13**(2) (1994) 121–131.
16. W. C. Shi, J. M. Zheng, Y. Li, X. B. Li and Q. N. An, Measurement and modeling of bidirectional reflectance distribution function (BRDF) on cutting surface based on the coaxial optical microscopic imaging, *Optik* **170**(10) (2018) 278–286.
17. N. Srichumroenrattana, R. Lipikorn and C. Lursinsap, Stereoscopic face reconstruction from a single 2-dimensional face image using orthogonality of normal surface and y-ratio, *Int. J. Pattern Recognit. Artif. Intell.* **30**(2) (2016) 1655006.
18. K. E. Torrance and E. M. Sparrow, Theory for off-specular reflection from roughened surfaces, *Opt. Soc.* **57**(3) (1967) 1105–1114.
19. G. H. Wang and J. Cheng, Three-dimensional reconstruction of hybrid surfaces using perspective shape from shading, *Optik.* **127**(19) (2016) 7740–7751.
20. A. G. Wang, J. Han, H. Jia and X. M. Zhang, Fast viscosity solutions for shape from shading under a more realistic imaging mode, *Opt. Eng.* **48**(11) (2009) 117201.
21. G. J. Ward, Measuring and modeling anisotropic reflection, *ACM SIGGRAPH Computer Graph.* **26**(2) (1992) 265–272.
22. Y. Hwang and J. Lee, Surface estimation ICP algorithm for building a 3D map by a scanning LRF, *Int. J. Pattern Recognit. Artif. Intell.* **14**(3) (2017) 1750011.
23. L. Zhao, C. H. Li, F. N. Dang, C. J. Li and Z. X. Duan, Concrete CT image quick three-dimensional reconstruction research, *Int. J. Pattern Recognit. Artif. Intell.* **31**(10) (2017) 1757005.

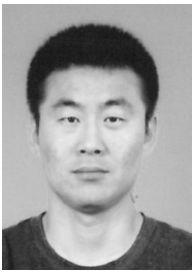

Weichao Shi received his B.S. degree in Mechanical Design manufacture and Automation from Northwest A&F University and his M.S. degree in Mechanical Engineering from Xi'an University of Technology, in 2003 and 2014, respectively. Currently, he is an Associate Professor at Xi'an University of Technology.

Jianming Zheng received his B.S. degree in Mechanical Design manufacture and Automation and his M.S. degree in Mechanical Engineering from Xi'an University of Technology, in 1990 and 1993, respectively, and his Ph.D. in Advanced manufacturing technology from Xi'an University of Technology in 2004. Currently, he is a professor and Ph.D. supervisor at Xi'an University of Technology.

Yan Li received his B.S. degree in Mechanical Design manufacture and Automation and his M.S. degree in Mechanical Engineering from Xi'an University of Technology, in 1983 and 1988, respectively, and his Ph.D. in Advanced manufacturing technology from Northwestern Polytechnical University in 1995. Currently, he is a Professor and Ph.D. supervisor at Xi'an University of Technology.

Xubo Li received his B.S. degree in Mechanical Design manufacture and Automation from Xi'an Polytechnic University and his M.S. degree in Mechanical Engineering from Xi'an University of Technology, in 2013 and 2016, respectively. Currently, he is a Ph.D Candidates at Xi'an University of Technology.

Qiannan An received his B.S. degree in Mechanical Design manufacture and Automation from Xi'an Technological University. Currently, she is a post graduate student at Xi'an University of Technology.